# Single-Sweep vs. Banded Characterizations of a D-band Ultra-Low-Loss SiC Substrate-Integrated Waveguide

Lei Li<sup>1</sup>, Steve Reyes<sup>2</sup>, Mohammad Javad Asadi<sup>1</sup>, Debdeep Jena<sup>1</sup>,
Huili Grace Xing<sup>1</sup>, Patrick Fay<sup>3</sup>, James C. M. Hwang<sup>1</sup>

<sup>1</sup>Cornell University, Ithaca, NY, USA, <sup>2</sup>Anritsu Co., Morgan Hill, CA, USA

<sup>3</sup>University of Notre Dame, South Bend, IN, USA

Abstract — A D-band (110–170 GHz) SiC substrate-integrated waveguide (SIW) is characterized on-wafer by two different vector network analyzers (VNAs): a 220-GHz single-sweep VNA and an 110-GHz VNA with WR8 (90–140 GHz) and WR5 (140–220 GHz) frequency extenders. To facilitate probing, the SIW input and output are transitioned to grounded coplanar waveguides (GCPWs). Two-tier calibration is used to de-embed the SIW-GCPW transitions as well as to extract the intrinsic SIW characteristics. In general, the two VNAs are in agreement and both result in an ultra-low insertion loss of approximately 0.2 dB/mm for the same SIW, despite stitching errors at band edges.

Index Terms — Calibration, microwave measurement, millimeter wave, on-wafer measurement, vector network analyzer.

#### I. INTRODUCTION

With the bandwidths of 6G wireless and other applications extending above 110 GHz, accurate and convenient characterization across the entire millimeter-wave band becomes necessary [1], [2]. However, conventional vector network analyzers (VNAs) can cover only up to 110 GHz in a single sweep and, above 110 GHz, waveguide-based frequency extenders are required for different bands. Questions then arise whether the discontinuities across bands of calibration and measurement are sufficiently accurate, considering multiple connections and contacts of different probes [3].

This work compares the characteristics of a D-band (110–170 GHz) SiC substrate-integrated waveguide (SIW) [4] measured on-wafer by two different VNAs: a newly available 220-GHz single-sweep VNA, and a 110-GHz VNA with WR8 (90–140 GHz) and WR5 (140–220 GHz) waveguide frequency extenders. The passive SIW device is expected to be linear and well suited for small-signal characterization. Its characteristics are predictable by 3D full-wave finite-element electromagnetic simulation. Its ultra-low (~ 0.2 dB/mm) in-band insertion loss and > 40 dB out-of-band return loss challenge measurements under both highly matched and highly mismatched conditions.

# II. EXPERIMENTS

# A. Device Design and Fabrication

Fig. 1(a) shows an 1100-µm-long SIW, fabricated in 100-µm-thick semi-insulating 6H SiC [4]. In addition to the top and bottom ground planes, the SIW is bound by two parallel rows of through-substrate vias (TSVs), with the two rows spaced

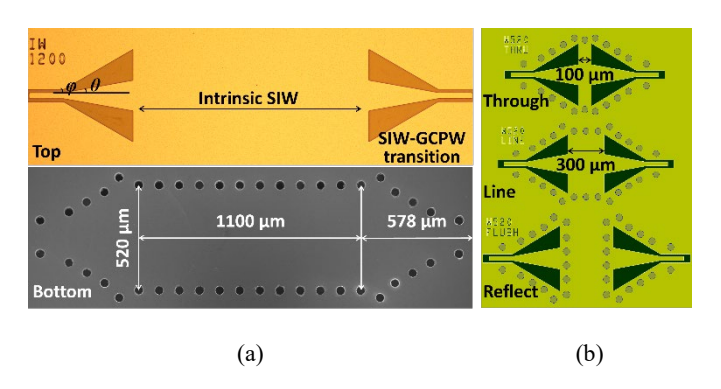


Fig. 1. (a) Front and back micrographs of a 1100-μm-long D-band SIW in series with two 578-μm-long SIW-GCPW transitions at the SIW input and output, respectively. (b) Composite layout of impedance standards: "through," "line," and "reflect" fabricated on the same SiC wafer [4].

520-µm apart center-to-center. Within each row, the TSVs are 50 μm in diameter and spaced by 100 μm center-to-center. For wafer probing, the SIW input and output are both transitioned to a grounded coplanar waveguide (GCPW). Each SIW-GCPW transition is 578-µm long, which includes a 175-µm GCPW section, a 353-um tapered section, and a 50-um SIW section [4]. In the GCPW section, the center electrode is 30-µm wide with a 16-µm gap from the ground electrodes. In the tapered section, the center electrode is linearly widened to 155 µm while the gap is linearly widened to 158 µm, corresponding to a tapered gap with  $\theta = 10^{\circ}$  and  $\varphi = 30^{\circ}$  for the inner and outer tapers, respectively. The transition has a low insertion loss (~ 0.2 dB) and a high return loss ( $\geq$  20 dB), which are critical to on-wafer characterization of the SIW. Otherwise, the measurement uncertainty would be dominated by that of the transition. After the above design is confirmed by the HFSS simulation, it is fabricated at Cornell University using precision semiconductor processes.

Both single-sweep and banded measurements involve two-tier calibrations. Tier-1 calibration establishes the reference plane at the probe tip 15  $\mu$ m from the outer edge of the GCPW, using a commercially available impedance standard substrate (ISS) fabricated in alumina. Tier-2 calibration moves the reference planes past the GCPW-SIW transitions by 50  $\mu$ m to the middle of "through" effectively rendering it zero-length, using impedance standards fabricated on the same SiC wafer as the SIW. Fig. 1(b) shows the layouts of "through," "line," and

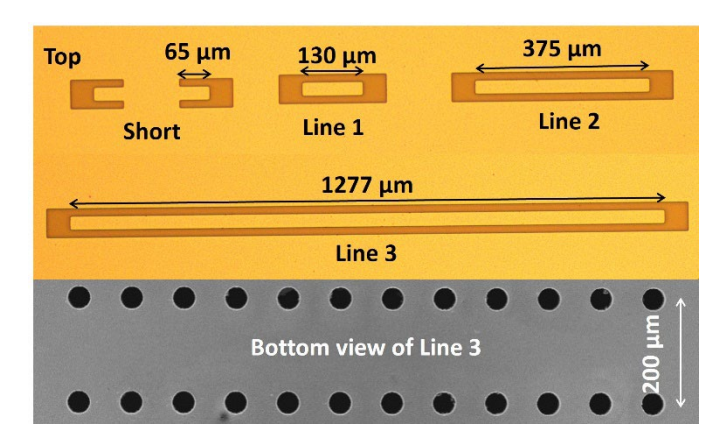


Fig. 2. Micrographs of GCPW lines of different lengths fabricated on the same SiC wafer as the SIWs.

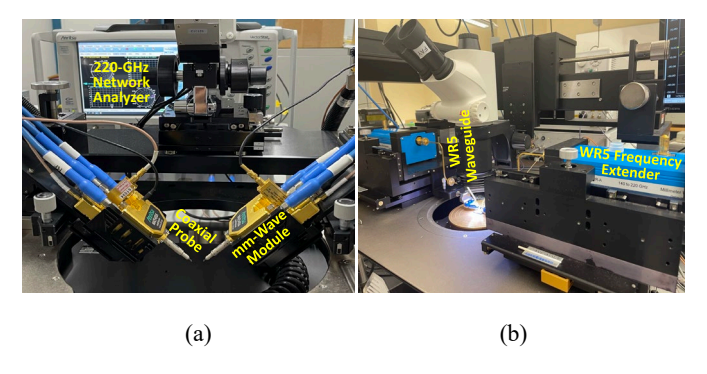


Fig. 3. Millimeter-wave wafer probing using (a) a 220-GHz single-sweep VNA and coaxial probes or (b) a 110-GHz VNA with waveguide-based frequency extenders and probes.

"reflect" standards, following the same design approach as that for the SIW. After tier-2 calibration, *S*-parameters of both intrinsic SIW and GCPW-SIW transitions are extracted.

To help validate the design and fabrication techniques, Fig. 2 shows GCPW lines of different lengths fabricated on the same SiC wafer as the SIWs. After the GCPWs are validated by tier-1 calibration using the commercial ISS, in the future, they can replace the commercial ISS for tier-1 calibration. This way, both tier-1 and tier-2 calibrations can be performed on wafer to further improve the calibration accuracy. Ultimately, with the GCPW-SIW transitions validated and repeatable, a single-tier calibration using the on-wafer impedance standards of Fig. 1(b) may be sufficient to extract the intrinsic SIW characteristics.

# B. Measurement Setups

Fig. 3 compares the setups for single-sweep and banded measurements. It can be seen in Fig. 3(a) that the single-sweep measurement is based on an Anritsu ME7838G 220-GHz VNA and two MPI TITAN 220-GHz coaxial probes with 50-μm pitch. Tier-1 calibration is based on an MPI TCS-050-100-W ISS and the load-reflection-match (LRM) method [5]. Tier-2 calibration is based on the on-wafer impedance standards of Fig. 1(b) and the through-reflect-line (TRL) method [6]. Fig. 3(b) shows that the banded measurement is based on a Keysight N5250A 110-GHz VNA plus pairs of VDI WR8 (90–140 GHz) and OML

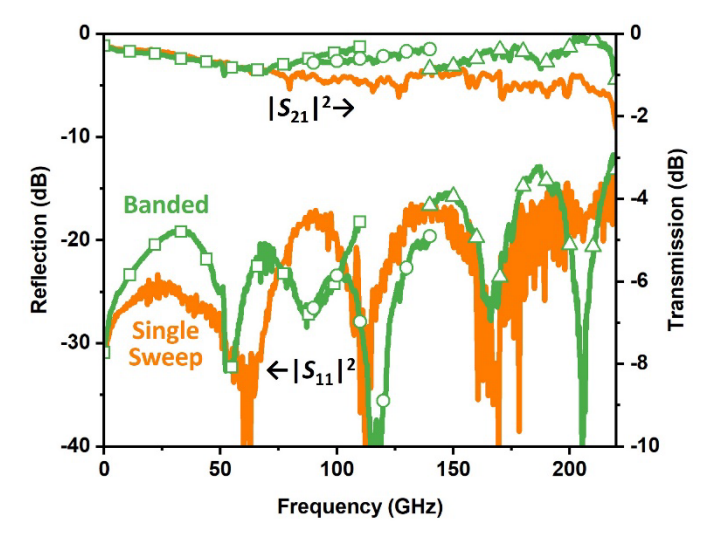


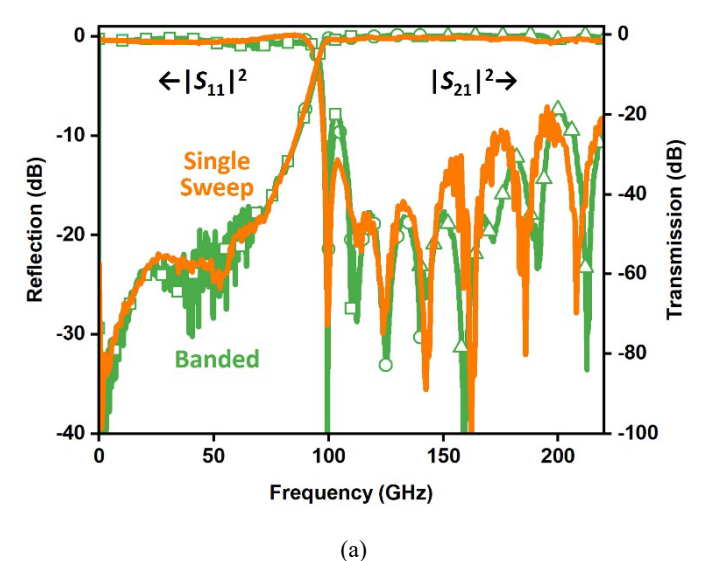
Fig. 4.  $S_{11}$  and  $S_{21}$  measured on an 1277- $\mu$ m-long GCPW in a single sweep from 0.1 to 220 GHz or in bands of 0.1–110 GHz ( $\Box$ ), 90–140 GHz ( $\Diamond$ ), and 140–220 GHz ( $\Delta$ ).

WR5 (140–220 GHz) waveguide frequency extenders. For each band, a different pair of FormFactor Infinity probes (I110-A-GSG-050, I140-T-GSG-050, and I220-T-GSG-050) are used. Tier-1 calibration is based on a FormFactor 138-356 ISS and the load-reflect-reflect-match (LRRM) method [5]. Tier-2 calibration is based on the on-wafer impedance standards and the TRL method, the same as that for the single-sweep measurement. Note that for on-wafer calibration, LRM and LRRM are more suitable for singe-sweep multi-decades measurements, whereas TRL is more suitable for banded measurements without precise definition of the matching impedance.

#### III. RESULTS AND DISCUSSION

## A. On-Wafer GCPW Lines

Fig. 4 compares from 0.1 GHz to 220 GHz the measured reflection coefficient  $S_{11}$  and transmission coefficient  $S_{21}$  of a 1277-µm-long GCPW line (Fig. 2) fabricated on the same SiC wafer as the SIWs, with the reference planes at the probe tips after tier-1 calibration. It can be seen that single-sweep and banded measurements give similar return losses, which validates the design and fabrication of the GCPW lines. However, while the single-sweep-measured insertion loss generally increases with increasing frequency as expected, the banded measurement above 67 GHz results in each band an insertion loss that decreases with increasing frequency. The variation in insertion loss over a band can be as large as 0.5 dB. A stitching error of this magnitude across bands is not uncommon for banded measurements [3]. This does not necessarily imply that the single-sweep LRM calibration is generally more accurate than the banded LRRM calibration. Rather, it suggests that our banded LRRM calibration should be improved. For example, multiple probe contacts are required



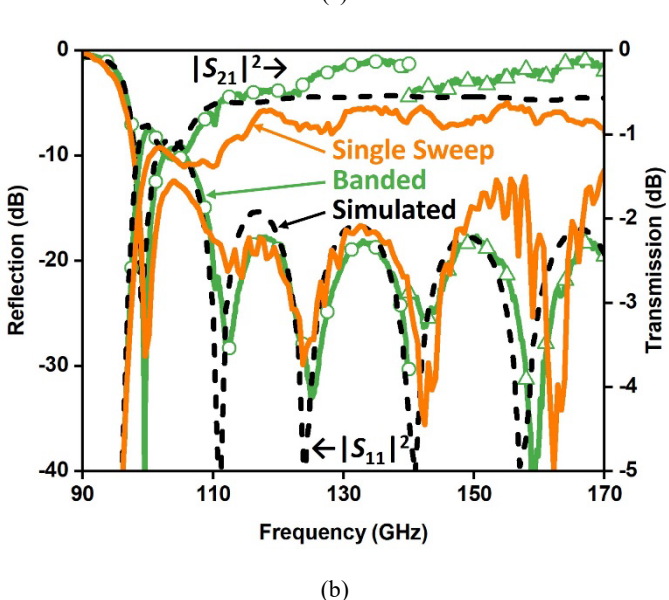


Fig. 5. (a)  $S_{11}$  and  $S_{21}$  measured on an 1100-µm-long SIW with GCPW input/output in (a) a single sweep from 0.1 to 220 GHz or in bands of 0.1–110 GHz ( $\Box$ ), 90–140 GHz ( $\circ$ ), and 140–220 GHz ( $\Delta$ ). (b) Expanded view of (a).

for the banded calibration and repeatable contacts are critical. However, our 0.7- $\mu$ m-thick Al pads tend to wear out with repeated probing, which can be reduced by using thicker and softer metal. Nevertheless, the above illustrates that single-sweep calibration is easier and more convenient than banded calibration.

## B. SIW with GCPW Input/Output

Fig. 5 compares measured  $S_{11}$  and  $S_{21}$  of a GCPW-SIW-GCPW series with a total length of 2.26 mm [Fig. 1(a)] and the reference planes at the probe tips after tier-1 calibration. It can be seen that single-sweep and banded measurements give similar return and insertion losses, even when the insertion loss approaches 100 dB. However, upon close examination [Fig.

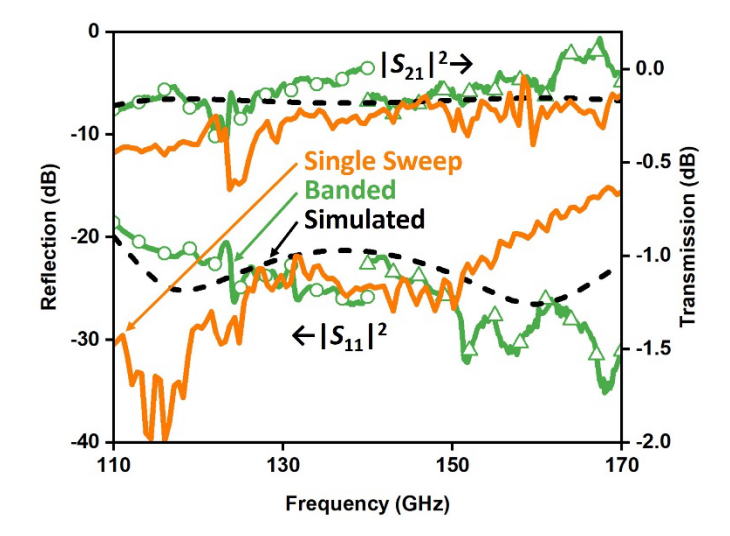


Fig. 6.  $S_{11}$  and  $S_{21}$  measured on an SIW-GCPW transition in a single sweep from 0.1 to 220 GHz or in bands of 90–140 GHz ( $\circ$ ) and 140–220 GHz ( $\Delta$ ).

5(b)], it can be seen that the single-sweep measurement gives a consistently higher insertion loss across the D band. In fact, the insertion losses by single-sweep and banded measurements are  $0.80 \pm 0.13$  dB and  $0.35 \pm 0.16$  dB, respectively. This can be attributed to the degradation of the probe pads on the SIW-GCPW transition as they are repeatedly probed, which leads to higher contact resistance (loss). Note that in this work we have repeated all measurements on the same SIW die, to avoid any additional uncertainty from die-to-die variation as the dies are fabricated in an academic facility.

Nevertheless, both single-sweep and banded measurements show that the return loss is greater than 17 dB across the D band, validating the design and fabrication of the SIW-GCPW transition. Additionally, the return loss of the single-sweep measurement exhibits more fine structure than that of the banded measurement, which can probably be improved by replacing the LRM calibration with the LRRM calibration to better correct the system directivity. The simulated insertion loss is between that of the single-sweep and banded measurements, probably because the simulation does not account for wear out. Furthermore, the simulated insertion loss coincides with the band-measured value at the lower band edge of 110 GHz or 140 GHz, before the band-measured value decreases with increasing frequency. This again suggests that our banded LRRM calibration needs to be improved.

## C. SIW-GCPW Transition

Fig. 6 compares the measured and simulated  $S_{11}$  and  $S_{21}$  of the SIW-GCPW transition de-embedded by the 2-tier calibration. The measured insertion losses are  $0.3 \pm 0.1$  dB and  $0.2 \pm 0.1$  dB by single-sweep and banded measurements, respectively. The 0.1-dB difference reflects the wear out by repeated probing. Meanwhile, the banded measurement results in insertion and return losses that decreases and increases with

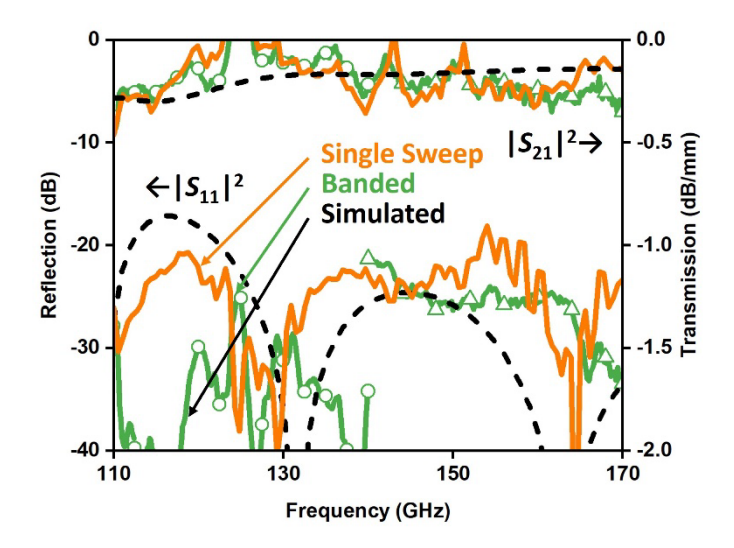


Fig. 7.  $S_{11}$  and  $S_{21}$  measured on an 1100-µm-long SIW in a single sweep from 0.1 to 220 GHz or in bands of 90–140 GHz ( $\circ$ ) and 140–220 GHz ( $\Delta$ ).

increasing frequency, respectively, similar to the case of a GCPW line as discussed in previous subsections.

#### D. Intrinsic SIW

Fig. 7 compares the measured and simulated  $S_{11}$  and  $S_{21}$  of the 1100-µm-long intrinsic SIW section, after tier-2 calibration and with the reference planes inside the GCPW-SIW transitions. It can be seen that across the D band, the simulation agrees with both the single-sweep and banded measurements. This shows that, unlike the SIW-GCPW transitions at the input and output, the intrinsic SIW is not affected by wear-out of the probe pads, as it is corrected by tier-2 calibration. Also, the problem of the banded tier-1 calibration is apparently corrected by the banded tier-2 calibration. As the result, the insertion loss is consistently  $0.2 \pm 0.1$  dB/mm and the reflection loss is greater than 20 dB for both single-sweep and banded measurement, validating the design, fabrication, and measurement of the SIW. For such an ultra-low loss SIW, the  $\pm$  0.1 dB measurement uncertainty appears inevitable and it is more important that the general trend is consistent with that simulated.

# IV. CONCLUSION

The above results confirm that accurate and consistent characterization across the millimeter-wave band is possible by both single-sweep and banded measurements, after careful calibration and de-embedding. This is important because while the single-sweep setup emerges, many banded measurement setups exist. Both the single-sweep and banded setups are expensive and skill-demanding, so not many labs can afford them. It is imperative to share the equipment, skills, and lessons learned.

#### ACKNOWLEDGMENT

This work is supported in part by the US National Science Foundation (NSF) under Grants ECCS-2117305 and ECCS-2122323, the US Office of Naval Research under Grant N00014-21-1-2680, as well as the Semiconductor Research Corporation and the US Defense Advanced Research Projects Agency through the Joint University Microelectronics Program. This work is performed in part at the Cornell NanoScale Facility, an NNCI member supported by NSF Grant NNCI-2025233.

## REFERENCES

- [1] U. Gustavsson *et al.*, "Implementation challenges and opportunities in beyond-5G and 6G communication," *IEEE J. Microw.*, vol. 1, no. 1, pp. 86–100, Jan. 2021.
- [2] W. Hong *et al.*, "The role of millimeter-wave technologies in 5G/6G wireless communications," *IEEE J. Microw.*, vol. 1, no. 1, pp. 101–122, Jan. 2021.
- [3] S. Fregonese, M. D. Matos, M. Deng, M. Potereau, C. Ayela, K. Aufinger, and T. Zimmer, "On-wafer characterization of silicon transistors up to 500 GHz and analysis of measurement discontinuities between the frequency bands," *IEEE Trans. Microw. Theory Techn.*, vol. 66, no. 7, pp. 3332–3341, Jul. 2018.
- [4] M. J. Asadi, L. Li, W. Zhao, K. Nomoto, P. Fay, H. G. Xing, D. Jena, and J. C. M. Hwang, "Substrate-integrated waveguides for monolithic integrated circuits above 110 GHz," in *IEEE MTT-S Int. Microwave Symp. (IMS)*, Atlanta, GA, Jun. 2021, pp. 669–672.
- [5] A. Davidson, K. Jones, and E. Strid, "LRM and LRRM calibrations with automatic determination of load inductance," in ARFTG Conf. Dig., Monterrey, CA, Nov. 1990, pp. 57–63.
- [6] R. B. Marks, "A multiline method of network analyzer calibration," *IEEE Trans. Microw. Theory Techn.*, vol. 39, no. 7, pp. 1205–1215, Jul. 1991.